Self-Assembly of L-Methionine on Cu(111): Steering Chiral Organization by Substrate Reactivity and Thermal Activation

Agustin Schiffrin,*,†,‡ Joachim Reichert,§,|| Yan Pennec,§ Willi Auwärter,§,|| Alexander Weber-Bargioni,§ Matthias Marschall,|| Martina Dell'Angela,⊥,# Dean Cvetko,▽ Gregor Bavdek,⊥,▽ Albano Cossaro,⊥ Alberto Morgante,⊥,# and Johannes V. Barth§,||

Department of Chemistry, The University of British Columbia, Vancouver, British Columbia V6T 1Z4, Canada, Max-Planck-Institut für Quantenoptik (MPQ), Hans-Kopfermann-Straβe 1, D-85748 Garching, Germany, Department of Physics & Astronomy, The University of British Columbia, Vancouver, British Columbia V6T 1Z4, Canada, Physik Department E20, Technische Universität München, D-85748 Garching, Germany, C.N.R.-INFM, Laboratorio Nazionale TASC, Trieste, Italy, Dipartimento di Fisica, Universita di Trieste, Trieste, Italy, and Physics Department, University of Ljubljana, Jadranska 19, SI-1000, Ljubljana, Slovenia

Received: January 20, 2009; Revised Manuscript Received: May 8, 2009

The self-assembly of the amino acid L-methionine on Cu(111) was investigated under ultrahigh vacuum (UHV) conditions by scanning tunneling microscopy (STM), helium atom scattering (HAS) and X-ray photoelectron spectroscopy (XPS). The system is strongly influenced by the substrate reactivity and the deposition temperature. The STM and HAS structural analysis yields that, for temperatures below 273 K, the biomolecules assemble in strings oriented with an angle of −10° with respect to the ⟨110⟩ axes of the substrate. For temperatures above 283 K, a regular and ordered one-dimensional (1D) phase arises following an angle of +10° with respect to the same directions. High resolution STM data of this ordered 1D arrangement evidence molecular dimerization and dimer alignment into ordered chains which are commensurate with the Cu(111) atomic lattice. XPS measurements reveal that the high temperature ordered phase consists of an exclusively anionic ensemble with a deprotonated carboxylic group and a neutral amino group, while the low temperature phase is heterogeneously composed of both zwitterionic and anionic species, depending on whether the molecules are immobilized in clusters of dimers on the free terraces or at the low-coordinated adsorption sites of the substrate step-edges. These combined results evidence a structural transformation of the supramolecular assembly which is triggered by a thermally activated process involving the underlying Cu(111) substrate and which carries the intrinsic chiral signature of the adsorbed molecular units.

I. Introduction

The fundamental investigation at the nanoscale of molecular self-assembly on surfaces comprises promising potential for the prospective design of functionalized interfaces. Notably, the adsorption of chiral species and the correlation with the mesoscopic enantiomorphic properties of their supramolecular self-assembly on a given substrate remains a challenging issue.[1−5] The pertaining understanding can provide critical insight into processes such as chiral recognition[5−8] and enantioselective catalysis in two dimensions.[5,9] With biologically relevant molecules, such as amino acids or nucleic acids, the elucidation of their adsorption on a surface and the translation of their chiral properties in two dimensions is a key to rationalize processes such as molecular recognition and chiral selectivity in biological systems.[6,10,11] Moreover, this understanding can lead to the evaluation of their self-assembly capabilities for potential noncovalent synthesis of functional two-dimensional nanostructures[1,12−14] and be useful for the prospective design of biocompatible materials.[15] Now, the configuration of a stable two-dimensional supramolecular ensemble at thermodynamic equilibrium is not only dictated by the lateral interactions between the adsorbed molecular entities, but also by the nature of the chemical and structural characteristics of the underlying support. Strong substrate-molecule interactions influence the diffusion properties of the adsorbed species, induce intramolecular conformational changes and even catalytically alter the chemical state of the molecules, having dramatic consequences on the supramolecular self-assembly configuration.[16−19] For instance, although in two dimensions the stereoselectivity between chiral species should increase due to the loss of dimensionality and therefore of degrees of freedom,[5,20] achiral supramolecular domains can emerge from the self-assembly of adsorbed chiral molecules due to strong chemisorption on specific substrate sites, as it is observed in the cases of the chiral amino acid alanine on Cu(110) and Cu(100).[1] Hence, the complex energy landscape of the adsorbate−substrate system is defined by its global thermodynamic conditions, and the enantiomorphic degrees of freedom of a final relaxed state of the self-assembled domain can be tuned by controlling external parameters such as temperature, as it has already been observed in previous thermally activated reversible chiral switching phenomena on surfaces.[21]

Scanning tunneling microscopy (STM) has shown unprecedented success for the determination of the local chiral properties of low-dimensional supramolecular self-assemblies

* To whom correspondence should be addressed. E-mail: agustin.schiffrin@mpq.mpg.de.
† Department of Chemistry, The University of British Columbia.
‡ Max-Planck-Institut für Quantenoptik (MPQ).
§ Department of Physics & Astronomy, The University of British Columbia.
|| Technische Universität München.
⊥ C.N.R.-INFM.
Universita di Trieste.
▽ University of Ljubljana.

10.1021/jp900593g CCC: $40.75
Published on Web 06/15/2009

at the molecular level.[22] Here we report a combined low-temperature STM (LT-STM), He atom scattering (HAS) and X-ray photoelectron spectroscopy (XPS) study on the self-assembly of the chiral amino acid L-methionine on Cu(111) in ultrahigh vacuum (UHV) conditions. Methionine provides functionalities which are both relevant for zwitterionic self-assembly and for metal binding sites in peptide chains. Our previous work[23] revealed that on Ag(111) this amino acid polymerizes and self-assembles in extended one-dimensional (1D) nanostructures running parallel to the close-packed crystallographic orientations of the underlying atomic lattice. These commensurate chains arrange mesoscopically into regular biomolecular gratings whose periodicity can be controlled by tuning the molecular coverage, as shown by topographic STM and HAS observations.[23] By contrast, on Cu(111) the molecular ordering is strongly influenced by the higher reactivity and the smaller lattice constant ($a_{Cu(111)} = 2.55$ Å; $a_{Ag(111)} = 2.89$ Å) of the substrate. At low temperatures (<273 K), irregular molecular strings evolve for submonolayer coverages, whereas the saturated monolayer exhibits partial ordering arising from the influence of the substrate symmetry, with linear structures growing with a $-10°$ (clockwise) tilt with respect to the ⟨110⟩ crystalline orientations. On the other hand, following deposition on the substrate held at temperatures above 283 K, a regular 1D phase arises oriented with an angle of $+10°$ with respect to the ⟨110⟩ axes coexisting with patches of the disordered low temperature phase. Molecular resolution STM measurements of the ordered 1D arrangement indicate dimerization and a second-order commensurability with the atomic lattice of the substrate along the chain direction. Long range ordering of the molecular clusters has been examined by HAS. He diffraction confirms that the low and high temperature L-methionine depositions yield two orientationally different phases, whereas for the intermediate substrate temperatures both phases coexist. XPS experiments additionally reveal that the high temperature ordered phase comprises the molecules in their anionic state, with a deprotonated carboxylic group and a neutral amino group. In contrast, the low temperature disordered phase reflects an heterogeneous zwitterionic ($CH_3SCH_2CH_2CH(NH_3)^+(COO)^-$) and anionic ($CH_3SCH_2CH_2CH(NH_2)(COO)^-$) self-assembly, whereby the anionic state is associated with metal−ligand binding of the amino acid molecules with the more reactive, less coordinated copper atoms at step-edges. It is concluded that the structural transformation which the supramolecular assembly undergoes from low to high temperature is triggered by a thermally activated chemical transformation which is mediated by the reactivity of the underlying Cu(111) substrate and which switches the adsorbed molecular units' chiral organization.

II. Experimental Section

The morphological and structural properties of the system were studied by means of STM and HAS. XPS provided the spectroscopic information for the chemical state of the biomolecular self-assembly. The STM experiments were performed at a base pressure below 2×10^{-10} mbar in a custom-designed ultrahigh vacuum (UHV) system comprising a commercial Besocke-type LT-STM[24,25] and standard tools for in situ sample preparation and characterization. The chemomechanically polished Cu(111) sample was prepared in situ by cycles of Ar^+ sputtering at an energy of 0.8 keV, followed by annealing at a temperature of 770 K. The L- and D-methionine amino acid (≥99.5%, Sigma-Aldrich) was deposited by thermal evaporation at a crucible temperature of approximately 370 K and with a deposition rate of the order of 1 monolayer (ML) per minute.

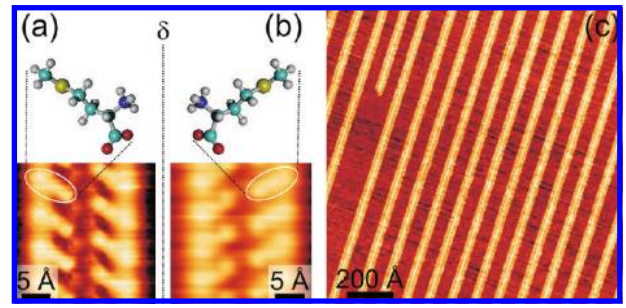

Figure 1. Self-assembly of the methionine amino acid on Ag(111). (a) Structural diagram of the L-methionine zwitterion and STM image of the molecular arrangement within its respective self-assembly ($I = 0.1$ nA, $U = -464$ mV). Color code: cyan (C), white (H), red (O), blue (N), and yellow (S). (b) D-Methionine zwitterionic enantiomer and STM image of the respective self-assembly: enantiomorphic noncovalent molecular bonding within the biomolecular nanostructure ($I = 0.1$ nA, $U = -80$ mV). (c) Homochiral L-methionine self-assembly forming regular and tunable 1D biomolecular nanogratings ($I = 0.1$ nA, $U = -500$ mV, $\theta = 0.38 \pm 0.08$ ML).

The morphology and chemical state of the molecular self-assembly were studied in dependence of the substrate temperature during the deposition, which was chosen between 240 and 320 K. Following the preparation, the sample was cooled down to temperatures below 15 K for the acquisition of the STM topographic data. The constant-current images were obtained with an electrochemically etched W tip and with the bias voltage applied to the sample. XPS and HAS measurements were performed at the ALOISA beamline[26] (ELETTRA synchrotron, Trieste, Italy), whereby deposition of methionine on Cu(111) was performed under the same UHV conditions as for the STM experiments. The HAS diffraction patterns were obtained with an incident He beam[27] of energy 19 meV and wavevector 6.3 $Å^{-1}$. The XP spectra were acquired with the sample cooled down to 193 K after preparation in order to minimize the radiation damage on the adsorbed biomolecular film.[28] The overall binding energy resolution is 300 meV with a photon energy of 596.7 eV.[26] The binding energy of the shown spectra is referenced to the substrate Fermi level. The XPS raw data was treated by subtracting the background signal due to inelastically scattered photoelectrons and by fitting with Voigt functions.

III. Results and Discussion

Our previous study of L-methionine deposited on Ag(111) showed that the amino acid adsorbs in its zwitterionic chemical state, forming regular 1D hydrogen-bonded nanogratings with tunable periodicity (Figure 1c).[23] On Ag(111), the chirality of the amino acid is reflected in the nonmirror-symmetric molecular arrangement within the supramolecular self-assembly: the L (D) enantiomer adsorbs with its long axis tilted with a $\sim+60°$ ($\sim-60°$) angle with respect to the substrate high-symmetry crystallographic orientation (Figure 1, panels a and b, respectively). However, this enantiomorphic organization of the zwitterions follows the substrate ⟨110⟩ axes, whence the homochiral self-assembly of D-methionine forms regular and tunable nanogratings with the same morphology as the L-methionine system. The enantiomorphism of such supramolecular chains recalls other 1D nanostructures arising however from the self-assembly of prochiral molecular units on the same substrate.[29,30]

On Cu(111), the picture is different due to the different lattice periodicity of this surface and moreover to the higher reactivity which can induce chemical transformations of the adsorbed

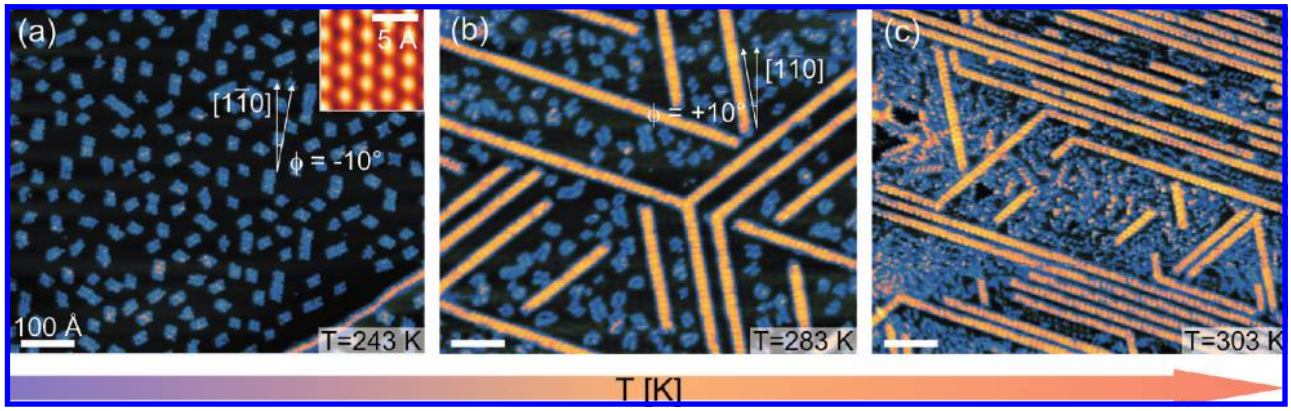

Figure 2. Homochiral L-methionine biomolecular self-assembly on Cu(111). (a) L-Methionine strings (α structure) following deposition on Cu(111) at $T = 243$ K ($I = 0.1$ nA, $U = -100$ mV, $\theta = 0.25 \pm 0.05$ ML). Inset: atomic resolution of the Cu(111) substrate. (b) At $T = 283$ K extended 1D chains emerge ($I = 0.1$ nA, $U = -100$ mV, $\theta = 0.42 \pm 0.05$ ML). (c) Deposition at T = 303 K ($I = 0.06$ nA, $U = -100$ mV, $\theta = 0.90 \pm 0.05$ ML) showing small domains of a nanograting (β structure). Scale bars: 100 Å.

species. Depending on the substrate temperature during the molecular deposition, methionine self-assembles into two distinct supramolecular structures which we label α and β. At 243 K, the molecules form short strings (Figure 2a), this pattern being defined as α structure. These formations grow following a 10° clockwise tilt with respect to the high-symmetry axes of the underlying lattice (e.g., [1$\bar{1}$0] surface direction). At higher substrate temperatures during deposition, an additional self-assembly pattern β arises. 1D arrays with long-range order emerge along an orientation rotated 10° counter-clockwise relative to the high-symmetry axes of the substrate (Figure 2b). Both phases coexist in a given temperature range, indicating a non trivial transition process between both entities. However, the ratio between the two phases is highly temperature dependent: at a higher temperature, the +10° rotated regular linear pattern prevails (Figure 2c).

HAS measurements have been performed to obtain an integral measure for the symmetry and long-range order of the biomolecular formations. As for the STM observations, the dependence of the system on the temperature during preparation was considered. The HAS 2D diffraction maps comprise orientational information on the supramolecular real space geometries on the surface. At temperatures below 280 K, a hexagonal diffraction pattern with blurred features and rotated 10° clockwise with respect to the <11$\bar{2}$> directions, perpendicular to the ⟨110⟩ axes of the Cu(111) substrate, indicates a partially ordered surface morphology which we associate with the phase α (Figure 3a). For higher sample temperatures, the diffraction features of the same sample preparation become better defined, which is visualized in Figure 3c. The increased biomolecular ordering at higher temperatures is also accompanied by a 20° counter-clockwise rotation of the diffraction hexagon (Figure 3, panels b and c), that is, oriented with a +10° angle with respect to the <11$\bar{2}$> directions, consistent with the formation of the β phase. For this regular phase, the STM real-space data reveal periodicities perpendicular to the linear biomolecular nanowires from ~25 to 50 Å depending on L-methionine coverage, in agreement with the appearance of the sharp satellite peaks in the HAS patterns (Figure 3c). Figure 3d illustrates the He diffraction intensity along the momentum line rotated 10° counter-clockwise from the <11$\bar{2}$> orientations (i.e., orientations within the surface plane perpendicular to the high-symmetry ⟨110⟩ substrate axes), which shows pronounced diffraction peaks up to sixth diffraction order. From the HAS peak widths we may estimate the biomolecular long-range correlation to exceed several hundreds of Ångstroms. The emergence of the highly

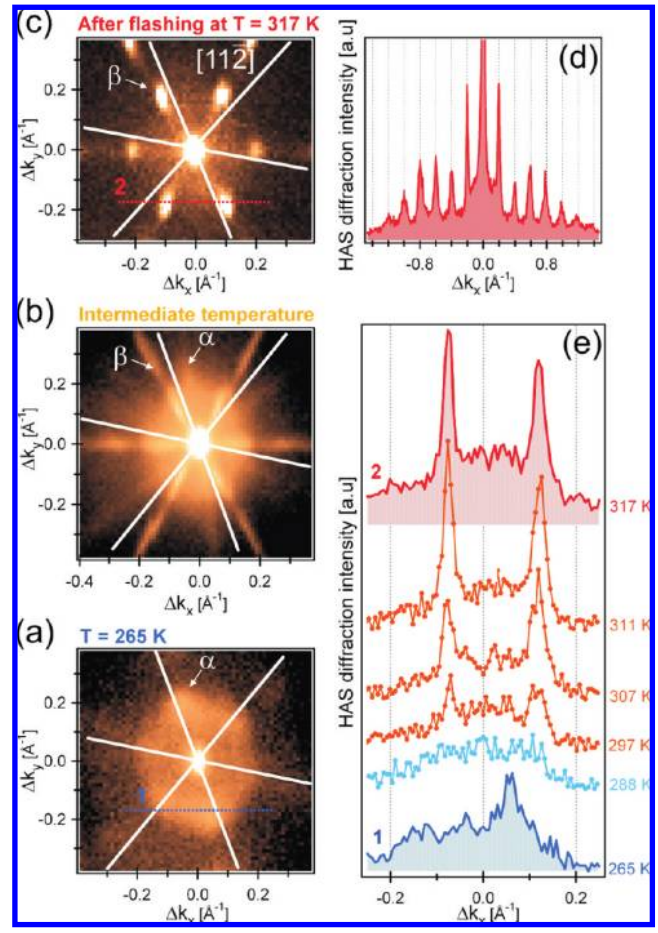

Figure 3. HAS data of the L-methionine/Cu(111) system. (a) Two-dimensional HAS diffraction map of the L-methionine/Cu(111) system for $T = 265$ K: well-developed hexagonal diffraction pattern with blurred features tilted clockwise by 10° relative to the <11$\bar{2}$> substrate directions (white lines), relative to the supramolecular phase α. (b) HAS diffraction map of the same sample preparation at intermediate temperature. Here the α and β supramolecular assembly phases coexist. (c) HAS diffraction map at 317 K: hexagonal pattern with pronounced satellite maxima and with a 10° counter-clockwise tilt relative to the <11$\bar{2}$> orientations of the substrate, associated with the supramolecular phase β. (d) 1D HAS diffraction pattern along the $\Delta k_y = 0$ line for the supramolecular phase β. (e) HAS intensity profiles along $\Delta k_y = -0.18 \pm 0.01$ Å^{-1} for substrate temperatures from 265 to 317 K: pronounced satellite maxima appear for temperatures above 288 K.

ordered phase in relation to substrate temperature is depicted in Figure 3e. It is important to point out that this structural transformation is not related to a change in molecular coverage, but it is purely controlled by the substrate temperature during molecular deposition. This observation is corroborated by STM and HAS data consistently obtained from preparations with different absorbate densities, and our XPS study on this system below explicitly showing that the change in morphology is triggered by a thermally activated chemical process.

The absence of the supramolecular configurations which are mirror symmetric to phases α and β with respect to the ⟨110⟩ crystallographic axes represent a break of symmetry of the system and is related to the chiral signature of the molecular building units. This demonstrates the role of the molecular reactive groups in the adsorption to the Cu(111) surface as well as of the intermolecular binding in the self-assembly of the supramolecular nanostructure. Such transfer of the molecular chiral 'footprint' into a mesoscopic supramolecular chirality has already been observed in previous studies of adsorbed amino acids or peptides on metal surfaces,[31−33] presenting a supplementary degree of morphological control on low-dimensional self-assembled nanostructures.

HAS and STM data agree on the orientational and morphological order on the local and mesoscopic length scales respectively, while the XPS data allows resolving the chemical state of the adsorbed molecules. The N 1s photoemission spectra were obtained close to a full monolayer L-methionine coverage. Spectra for the C 1s, S 2p and O 1s core electrons were also measured, the S 2p and O 1s signal showing no dependence on the sample temperature during deposition. The O 1s signature reveals a single peak at a binding energy of $E_{O1s} = 531.5 \pm 0.1$ eV, which corresponds to the deprotonated oxygen atoms of the resonating amino acid carboxylate group, and which is similar to the O 1s binding energy of 531.2 eV measured for the carboxylate group oxygen atoms in the L-methionine/Ag(111) system.[23] Here, the discrepancy of 0.3 eV between the Cu(111) and Ag(111) cases may point to different screening of the molecular charge distribution by the substrate polarizability, this difference being due to a different molecular adsorption geometry on both surfaces. On Cu(111), the increased O 1s binding energy may indicate a slightly larger distance between the carboxylate group and the surface. Such chemical shifts due to a different local geometric environment have already been mentioned in studies concerning the adsorption of glycine on Cu(110).[34]

The case of the N 1s analysis is more complex and the related spectra are shown in Figure 4. For a substrate temperature of 265 K during deposition, we find two distinct peaks: one at a binding energy of $E^{(1)}_{N1s} = 399.5 \pm 0.2$ eV, another one at $E^{(2)}_{N1s} = 401.3 \pm 0.1$ eV. XPS data acquisition with 1s time resolution demonstrated that the two components are intrinsic to the supramolecular assembly deposited at 265K and are not an artifact of the photon beam exposure. By comparing with XPS experiments performed on the L-cysteine/Au(110)[35] and L-methionine/Ag(111)[23] systems, we deduce that $E^{(1)}_{N1s}$ corresponds to the amino group NH_2, whereas $E^{(2)}_{N1s}$ is assigned to the ammonium group NH_3^+. After annealing the same sample above ~320 K, only the $E^{(1)}_{N1s}$ peak at 399.5 eV can be detected. The observed morphological and orientational switch from the α to the β phase hence involves the signature of a chemical transformation occurring on the nitrogen-containing group. Whereas N 1s XPS of the low temperature phase predominantly evidence the NH_3^+ group, the system heated to 320 K shows a distinct signature exclusively of the NH_2 moiety.

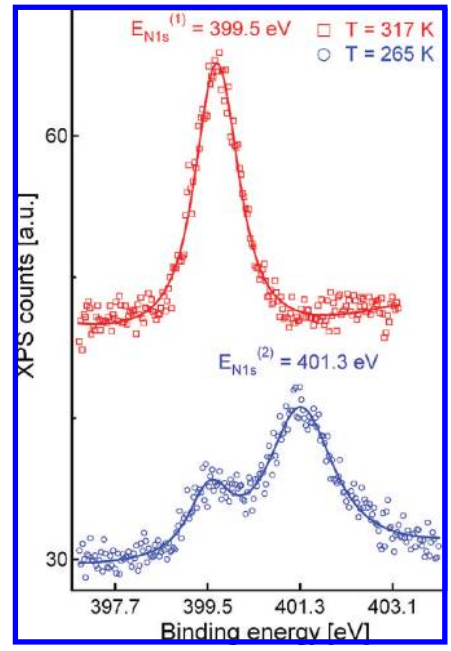

Figure 4. N 1s XP spectra of L-methionine on Cu(111) for the low (blue) and high (red) temperature phases: the phase transition from α to β is associated to the deprotonation of the ammomium group. High temperature spectrum shifted upward for clarity.

Taking into account that the O 1s spectrum represents the chemical trace of the carboxylate group, we conclude that at low temperatures zwitterionic and anionic molecules coexist, whereas the high temperature phase is composed of purely anionic species. Our measurements clearly show that the thermally activated phase switch involves a chemical process where the ammonium group NH_3^+ of the zwitterionic portion deprotonates.

For the low temperature biomolecular self-assembly, however, the dual chemical composition is more intricate. Figure 5, panels a and b, focuses on the pertaining XPS N 1s peaks for a sample preparation temperature of 233 K. The inset in Figure 5a represents the ratio r between the areas of the Voigt curves fitting N $1s^{(2)}$ and N $1s^{(1)}$ respectively, depending on the molecular coverage θ. The molecular coverage was obtained from the overall XPS N 1s intensity combined with the HAS specular measurements during L-methionine deposition: the relative molecular coverage is estimated from the total N 1s integrated intensity (N $1s^{(1)}$ and N $1s^{(2)}$), whereas the attenuation of HAS specular intensity monitors the portion of L-methionine covered Cu substrate. Complete disappearance of HAS specular intensity is assigned to a saturated molecular monolayer (i.e., $\theta = 1$ ML). It becomes clear that there is a relative increasing term trend of r with respect to θ, meaning that there is an increase of the zwitterionic species with coverage. Morphologically, it has been observed in the STM data that the molecules, having enough thermal energy to diffuse at the deposition temperature (for high as well as for the low temperature cases), bind first to the substrate step-edges, where the Cu atoms are less coordinated and therefore their interaction with the biomolecules is stronger. This indicates that the amino acid molecules bind to the substrate step-edges are in their anionic form and are related to the XPS N $1s^{(1)}$ peak. Once there are enough species to saturate the step-edges, the zwitterionic strings emerge. The intensity of the XPS N $1s^{(2)}$ peak increases once the molecules have decorated the step edges. The STM image in Figure 5c shows the decoration of the step-edges by the biomolecules for the low temperature case, indicated by the white arrows. This hypothesis is cor-

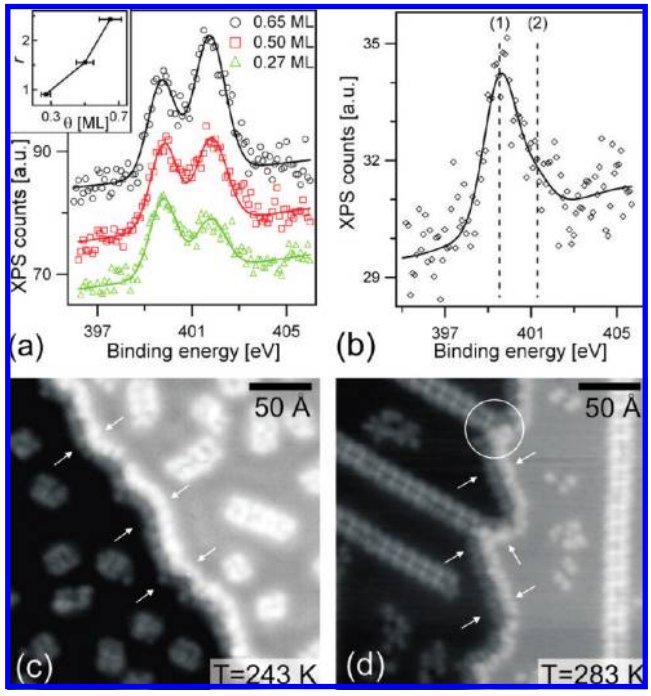

Figure 5. Dependence of the XP N 1s spectra on the molecular coverage θ and on step-edge density for the low temperature phase. (a) Variation of the relative intensity of XPS peaks N $1s^{(1)}$ and N $1s^{(2)}$ for different submonolayer coverages θ for the low temperature phase: relative intensity of the N $1s^{(2)}$ peak increases with molecular coverage. Inset: ratio r between the area of the Voigt curves for peaks N $1s^{(2)}$ and N $1s^{(1)}$ as a function of θ. (b) N 1s XP spectrum for a higher step-edge density and molecular coverage θ of 0.16 ± 0.05 ML: Voigt fit shows a relatively high N $1s^{(1)}$ peak at position (1), corresponding to a high number of molecules bonded to the substrate step-edges, whereas N $1s^{(2)}$ peak at position (2) is not observed. (c) STM topographic image ($I = 0.1$ nA, $U = -200$ mV) of phase α prepared at 243 K shows the biomolecules bonded to the step-edges (white arrows) related to the N $1s^{(1)}$ XPS peak. (d) STM topographical image ($I = 0.1$ nA, $U = -500$ mV) of phase β prepared at 283 K: the step-edges are perturbed by the bonded molecular species (white arrows) and the nucleation of the ordered molecular phase is linked to the low-coordinated adsorption sites (white circle).

roborated in the XPS N 1s spectrum in Figure 5b, where a substrate with a higher density of step-edges was considered for the low temperature molecule deposition with a molecular coverage θ of 0.16 ± 0.05 ML. Such a rough surface was obtained by Ar^+ sputtering at 0.3 keV after the usual cleaning procedure of the sample. The reduced surface order was monitored by HAS specular reflectivity as well as specular peak width. Here, the N $1s^{(2)}$ peak related to the ammonium group (position (2) in Figure 5b) is almost undetectable, whereas the amino group N $1s^{(1)}$ peak at 399.5 eV clearly prevails, revealing that zwitterionic L-methionine species dominate over anionic ones only for a well ordered Cu(111) substrate, that is, a substrate presenting large flat (111) terraces and a low step-edge density.

Thus, on a flat Cu(111) terrace the deprotonation of the ammonium group takes above 283 K, the XPS data relative to the highly ordered high temperature phase β revealing exclusively an anionic moiety, whereas on a surface presenting a high density of step-edges this process is already observed at 265 K. From these observations, and in comparison with the case of Ag(111), the Cu surface triggers the deprotonation of the ammonium group, the temperature dependent characteristics of this chemical process evidencing a lower activation barrier at the step-edges. The anionic chemical state with a neutral amino group and a negatively charged carboxylate group for the high temperature phase is identical to the chemical configuration of other amino acids such as alanine and glycine adsorbed on low-index Cu surfaces at room temperature.[36−39] In these previous experimental[37,38] and theoretical[40,41] studies, it was shown that the amino acids bind to the metal substrate through their amino and carboxylate groups, the nitrogen and oxygen atoms preferentially sitting near atop sites of the Cu crystal. Here our work indicates that the binding of the biomolecule through its N atom is enabled by the thermally activated deprotonation of the ammonium group and reveals the directing role of the Cu substrate on the supramolecular chemistry and morphology. This influence of the Cu(111) surface is emphasized by reminding here that the XPS study of the same molecule adsorbed on the less reactive Ag(111) surface[23] revealed a temperature independent zwitterionic chemical state of the adsorbate, with no evidence of increased reactivity of the low coordinated Ag atoms at the step-edges.

Moreover, we observed that the thermal excitation of the system not only triggers a chemical process: in addition, the morphology of the substrate step-edges is altered by the amino acid adsorption, becoming indented, as seen in Figure 5d. This adsorbate induced step-edge faceting phenomenon has been already observed for related amino acids adsorbed on Cu surfaces,[42−44] as well as for carboxylate units on Ag surfaces.[45] Additionally, one can observe that the nucleation of the ordered 1D assembly at high temperature is linked to the perturbation of the step edges by the molecular adsorption and that this highly ordered phase is in fact an extension of the molecules decorating the step edges, giving supplementary evidence that these species are likely to be chemically identical.

From the real space topographic perspective, the low temperature STM data allow resolving the molecular arrangement of both phases. Figure 6a shows details within the α phase strings and reveal supramolecular polymerization in the form of twin chains. The apparent height of these α phase clusters measured with STM is 1.2 ± 0.1 Å and does not vary in the range from −500 to +500 mV of applied bias voltages. The XPS measurements having demonstrated that this phase corresponds to the self-assembly of the amino acid molecules in their zwitterionic state, we can assume that the intermolecular bonding scheme is similar to the one found in the L-methionine/Ag(111) system, the 10° clockwise rotation with respect the ⟨110⟩ orientations being necessary to match the energetically favorable adjacent intermolecular distance to the smaller lattice constant of the Cu(111) substrate. In contrast to the highly linear regularity of the gratings found on Ag(111), systematic parallel adsorption of the molecular species cannot be concluded within the zwitterionic α-phase assembly on Cu(111) and only restrained 1D extensibility is shown. This could be related to the reduced mobility and higher nucleation density of the adsorbate on the more reactive Cu(111) substrate, which would kinetically limit the self-assembly process. The STM topograph of phase α in Figure 6a reveals a substantially disordered intrachain molecular arrangement and a nonunique geometrical configuration of the adsorbed molecule within the self-assembled clusters. Nevertheless, the zwitterionic nature of this phase along with the tendency of the amino acid to dimerize along its long axis in a non perfectly parallel fashion suggests a model of chain formation similar to the case of L-methionine on Ag(111).[23] In this low temperature case, a perfectly ordered self-assembly is hindered by the aforementioned kinetic limitations imposed by the substrate periodicity, symmetry and reactivity.

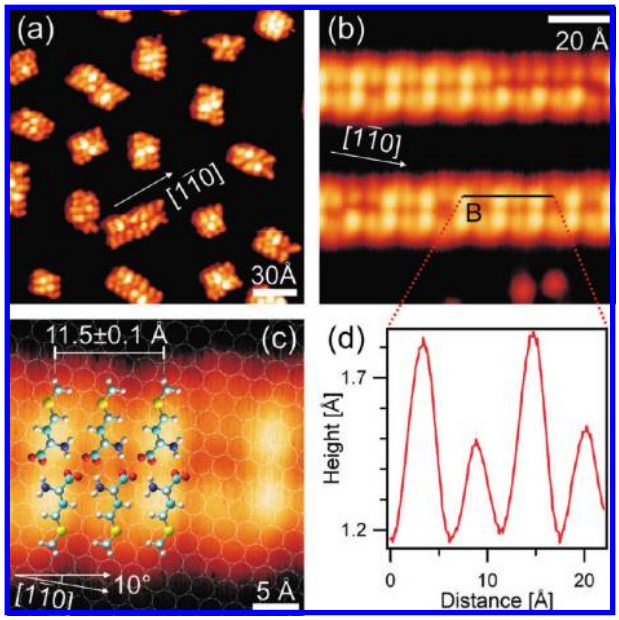

Figure 6. Molecular resolution STM data of phases α and β. (a) The α phase strings comprise a twin-chain motif and are tilted 10° clockwise off the substrate ⟨110⟩ orientations ($I = 0.1$ nA, $U = -100$ mV). (b) In the regular β phase tilted 10° counterclockwise off the substrate ⟨110⟩ orientations, whereby every second molecule shows the same apparent height, revealing equivalent adsorption sites on the substrate ($I = 0.1$ nA, $U = -600$ mV). (c) Model of the molecular arrangement within the β phase superimposed on an STM image with the underlying atomic lattice illustrated by white circles. The biomolecular nanostructure is commensurate with the substrate atomic periodicity. ($I = 0.1$ nA, $U = -600$ mV). (d) Apparent height profile along line B in (b) reveals the second order commensurability.

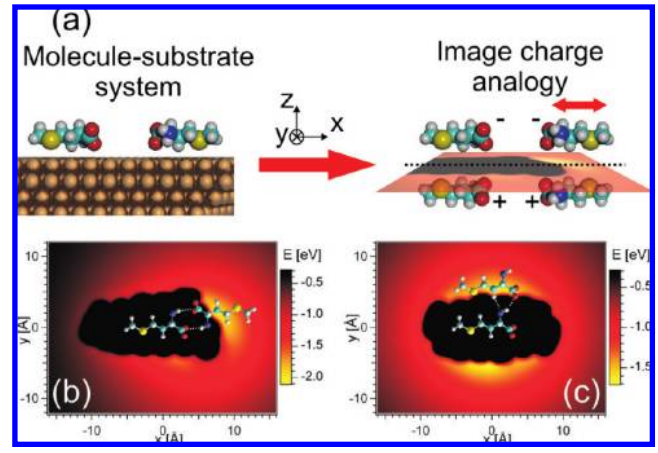

Figure 7. Molecular mechanics calculations for the ordered anionically composed phase β. (a) The two-molecule L-methionine system adsorbed on Cu(111) is considered as a 4-molecule system: the two real L-methionine molecules and 2 virtual D-methionine molecules of opposite charge are placed symmetrically with respect to the plane defined by the substrate. (b) Two-dimensional interaction energy landscape of the molecular system in the antiparallel configuration: minimum energy position implies H-bonded head-to-head dimerization. (c) Interaction energy landscape in the parallel configuration: adjacent H-bonding motif supports long-range 1D order.

On the other hand, the anionic phase β (Figure 6, panels b and c) shows extended 1D order and a 10° counterclockwise tilt relative to the ⟨110⟩ orientations of the substrate revealing a chiral switching process of the nanostructures. The rows in this phase are composed of strings of parallel dimers. It becomes clear in the high resolution STM images that the regularity in this dimer arrangement is significantly higher. Along the growth direction, a second-order commensurability pattern becomes evident (Figure 6b), visualized by the height profile on Figure 6d along line B. The brightest molecules on the STM topographs in Figure 6, panels b and c, have a bias-independent apparent height of 1.8 ± 0.1 Å in the bias voltage range of −600 to +600 mV, and adjacent dimers appear with an apparent height difference of ∼0.3 Å, every second dimer showing the same features. This contrast pattern can be explained with an atomistic model of the molecule−substrate system (Figure 6c). With the periodicity of 5.8 Å given by the STM data and the 10° tilt counter-clockwise to the ⟨110⟩ axes, every second dimer exhibits the same adsorption site. The in-row periodicity is remarkably close to the one found in L-methionine/Ag(111) system, and hence the tilt can be an adjustment to match the smaller lattice constant of 2.55 Å of the Cu(111) surface. This adjustment within the molecular arrangement is related to specific binding sites of the different amino acid functional groups with respect to the underlying atomic lattice. The Moiré pattern observed in the STM data would therefore be explained by a different electronic coupling of the amino acid to different adsorption sites of the substrate. Apparent height differences with the same order of magnitude have already been noticed for other organic molecules adsorbed on Cu(111)[46] and inorganic alloy superlattices on Au(111).[47] Our results could therefore hint an adsorption scenario similar to the cases of alanine and glycine on copper surfaces,[37,38,40,41] which, as aforementioned, yield specific binding through the N and O atoms of the ammonium and carboxylate groups near atop sites of the copper atomic lattice. The molecular dimerization and the topographic characteristics of the self-assembly shown by the STM images suggest a hydrogen-bond driven head-to-head assemblage between two molecules along their main axis, where one of the negatively charged oxygen atoms of the carboxylate group faces an amino hydrogen atom. The linear growth can be explained by adjacent H-bonding involving again the carboxylate and amino groups. The proposed bonding scheme is related to the one of the L-methionine/Ag(111) system.[23]

The high regularity of phase β allows us to examine its binding scheme in more detail. The XPS experiments having revealed that the species in this phase are anionic, a question remains concerning how an attractive interaction is possible between negatively charged entities. The polarizability of the metallic substrate plausibly enables the assembly process by screening the molecular negative charge through charge density redistribution. To reinforce the interpretation of the data as due to the head-to-head dimerization and the adjacent H-bonding in our atomistic model, molecular mechanics simulations were conducted. We considered a system composed of two L-methionine molecules, whose interacting energy was determined using a MM+[48] force field approach. To qualitatively include the screening effect of the substrate, image charges were included in our model by placing oppositely charged mirrored molecules below the Cu(111) surface plane (Figure 7a). The presence of the image charges in this simplified model of the molecules-substrate system results in an attractive intermolecular interaction. This is depicted in Figure 7, panels b and c, where we observe energy minima in the two-dimensional interacting energy landscape of the system. Figure 7b corresponds to the antiparallel molecular configuration, indicating that head-to-head dimerization is energetically favorable. The calculation of the interaction energy landscape for the parallel configuration is illustrated in Figure 7c, suggesting bonding of adjacent dimers

driving the linear extensibility of the nanostructures. This simplified image charge calculation endorses the proposed model of the molecular arrangement in phase β.

Whereas this molecular mechanics approach aims to explain the local intermolecular binding scheme within the supramolecular nanostructures of phase β, the regular mesoscopic ordering of this phase observed in our STM data (Figure 2c) and corroborated by the HAS experiments (Figure 3) could be the effect of long-range indirect interactions mediated by the Cu(111) surface electronic structure. In fact, low-temperature scanning tunneling spectroscopy measurements performed within this study revealed that the self-assembled biomolecular chains scatter and confine the Cu(111) Shockley surface-state electrons in a way similar to the previously studied L-methionine/Ag(111) system.[49] The scattering of the surface-state electrons by adsorbed species gives rise to an oscillatory long-range interaction[50] which has already been assigned as a determining factor in the self-ordering of adatoms into 1D atomic chains[51] and 2D atomic lattices,[52−55] and in the self-assembly of organic molecules[56,57] on close-packed noble metal surfaces. In comparison with the case of Ag(111), this substrate-mediated interaction in the L-methionine/Cu(111) system could be stronger due to a larger surface-state electronic density given by an electron effective mass of $0.38 \pm 0.02\ m_e$ (m_e being the electron mass) and a surface-state band onset situated at -0.44 ± 0.01 eV with respect to the Fermi level[58] and could therefore play an important role in the mesoscopic ordering of the self-assembled 1D nanostructures.

The results above present a scenario where the thermally activated ammonium deprotonation is the mediation for the orientational transformation between the low and high temperature cases. The low temperature preferential orientation of the supramolecular arrangement along a 10° clockwise tilt with respect to the ⟨110⟩ high-symmetry axes represents already an adsorbate induced break of the 3-fold symmetry imposed by the surface crystalline structure: the molecular chiral signature leads to an enantiomorphic organization reflecting a preferential adsorption configuration. Work by Weigelt et al.[21] showed chiral switching due to thermally driven conformational changes of individual molecular units, whereas our system is characterized by collective chiral switching mediated by a thermally activated chemical transformation. The ammonium deprotonation reassigns a preferential adsorption configuration, and the chiral properties of the system are altered accordingly.

IV. Conclusions

In conclusion, the self-assembly of the L-methionine amino acid on Cu(111) was comprehensively resolved, in terms of morphology through STM and HAS measurements, but also in terms of its chemistry through XPS experiments. The main point of this study resides in the supplementary parameter of control on the biomolecular nanostructures: the thermal activation of the system triggers a chemical process which dramatically alters the final organization and enantiomorphic ordering of the self-assembly. Here, the chemical reactivity of the Cu(111) substrate induces a thermally activated deprotonation of the amino acid ammonium group, which drives a morphological chiral switching process within the biomolecular ensemble and reveals an entirely new supramolecular configuration. The underlying crystal, through its structural and chemical properties, plays a key role in the equilibrium outcome of the self-assembly process.

Acknowledgment. This work was financially supported by NSERC, CFI, DFG, SNF, and the DAAD. The software package HyperChem 7.5 was used (Hyperchem(TM) Professional 7.51, Hypercube, Inc., 1115 NW fourth Street, Gainesville, Florida 32601, USA) for the MM+ force field calculations. We thank Roman Fasel for his help with the computational procedures for these calculations.

References and Notes

(1) Barlow, S. M.; Raval, R. *Surf. Sci. Rep.* **2003**, *50*, 201–341.
(2) Fasel, R.; Parschau, M.; Ernst, K. H. *Angew. Chem., Int. Ed.* **2003**, *42*, 5178–5181.
(3) Stepanow, S.; Lin, N.; Vidal, F.; Landa, A.; Ruben, M.; Barth, J. V.; Kern, K. *Nano Lett.* **2005**, *5*, 901–904.
(4) Xu, B.; Tao, C. G.; Cullen, W. G.; Reutt-Robey, J. E.; Williams, E. D. *Nano Lett.* **2005**, *5*, 2207–2211.
(5) Ernst, K. H. *Top. Curr. Chem.* **2006**, *265*, 209–252.
(6) Kühnle, A.; Linderoth, T. R.; Hammer, B.; Besenbacher, F. *Nature* **2002**, *415*, 891–893.
(7) Fasel, R.; Parschau, M.; Ernst, K. H. *Nature* **2006**, *439*, 449–452.
(8) Gladys, M. J.; Stevens, A. V.; Scott, N. R.; Jones, G.; Batchelor, D.; Held, G. *J. Phys. Chem. C* **2007**, *111*, 8331–8336.
(9) Nilsson, A.; Pettersson, L. G. M. *Surf. Sci. Rep.* **2004**, *55*, 49–167.
(10) Chen, Q.; Richardson, N. V. *Nat. Mater.* **2003**, *2*, 324–328.
(11) Blankenburg, S.; Schmidt, W. G. *Phys. Rev. Lett.* **2007**, *99*, 196107.
(12) Otero, R.; Schock, M.; Molina, L. M.; Laegsgaard, E.; Stensgaard, I.; Hammer, B.; Besenbacher, F. *Angew. Chem. Int. Ed.* **2005**, *44*, 2270–2275.
(13) Barth, J. V.; Costantini, G.; Kern, K. *Nature* **2005**, *437*, 671–679.
(14) Barth, J. V. *Annu. Rev. Phys. Chem.* **2007**, *58*, 375–407.
(15) Wolner, C.; Nauer, G. E.; Trummer, J.; Putz, V.; Tschegg, S. *Mater. Sci. Eng. C* **2006**, *26*, 34–40.
(16) Auwarter, W.; Weber-Bargioni, A.; Riemann, A.; Schiffrin, A.; Groning, O.; Fasel, R.; Barth, J. V. *J. Chem. Phys.* **2006**, *124*, 194708.
(17) Auwarter, W.; Klappenberger, F.; Weber-Bargioni, A.; Schiffrin, A.; Strunskus, T.; Woll, C.; Pennec, Y.; Riemann, A.; Barth, J. V. *J. Am. Chem. Soc.* **2007**, *129*, 11279–11285.
(18) Ghiringhelli, L. M.; Delle Site, L. *J. Am. Chem. Soc.* **2008**, *130*, 2634–2638.
(19) Rauls, E.; Schmidt, W. G. *J. Phys. Chem. C* **2008**, *112*, 11490–11494.
(20) Kuzmenko, I.; Weissbuch, I.; Gurovich, E.; Leiserowitz, L.; Lahav, M. *Chirality* **1998**, *10*, 415–424.
(21) Weigelt, S.; Busse, C.; Petersen, L.; Rauls, E.; Hammer, B.; Gothelf, K. V.; Besenbacher, F.; Linderoth, T. R. *Nat. Mater.* **2006**, *5*, 112–117.
(22) Lopinski, G. P.; Moffatt, D. J.; Wayner, D. D.; Wolkow, R. A. *Nature* **1998**, *392*, 909–911.
(23) Schiffrin, A.; Riemann, A.; Auwarter, W.; Pennec, Y.; Weber-Bargioni, A.; Cvetko, D.; Cossaro, A.; Alberto, M.; Barth, J. V. *Proc. Natl. Acad. Sci. U.S.A.* **2007**, *104*, 5279–5284.
(24) Meyer, G. *Rev. Sci. Instrum.* **1996**, *67*, 2960.
(25) http://www.lt-stm.com/.
(26) Floreano, L.; Naletto, G.; Cvetko, D.; R. G.; Malvezzi, M.; Marassi, L.; Morgante, A.; Santaniello, A.; Verdini, A.; Tommasini, F.; Tondello, G. *Rev. Sci. Instrum.* **1999**, *70*, 3855.
(27) Cvetko, D.; Lausi, A.; Morgante, A.; Tommasini, F.; Prince, K. C.; Sastry, M. *Meas. Sci. Technol.* **1992**, *3*, 997–1000.
(28) Feulner, P.; Niedermayer, T.; Eberle, K.; Schneider, R.; Menzel, D.; Baumer, A.; Schmich, E.; Shaporenko, A.; Tai, Y.; Zharnikov, M. *Phys. Rev. Lett.* **2004**, *93*, 178302.
(29) Weckesser, J.; Vita, A. D.; Barth, J. V.; Cai, C.; Kern, K. *Phys. Rev. Lett.* **2001**, *87*, 096101.
(30) Barth, J. V.; Weckesser, J.; Trimarchi, G.; Vladimirova, M.; Vita, A. D.; Cai, C.; Brune, H.; Günter, P.; Kern, K. *J. Am. Chem. Soc.* **2002**, *124*, 7991–8000.
(31) Barlow, S. M.; Louafi, S.; Le Roux, D.; Williams, J.; Muryn, C.; Haq, S.; Raval, R. *Surf. Sci.* **2005**, *590*, 243–263.
(32) Lingenfelder, M.; Tomba, G.; Costantini, G.; Ciacchi, L. C.; De Vita, A.; Kern, K. *Angew. Chem. Int. Ed.* **2007**, *46*, 4492–4495.
(33) Tomba, G.; Lingenfelder, M.; Costantini, G.; Kern, K.; Klappenberger, F.; Barth, J. V.; Ciacchi, L. C.; De Vita, A. *J. Phys. Chem. A* **2007**, *111*, 12740–12748.
(34) Hasselstrom, J.; Karis, O.; Weinelt, M.; Wassdahl, N.; Nilsson, A.; Nyberg, M.; Pettersson, L. G. M.; Samant, M. G.; Stohr, J. *Surf. Sci.* **1998**, *407*, 221–236.
(35) Gonella, G.; Terreni, S.; Cvetko, D.; Cossaro, A.; Mattera, L.; Cavalleri, O.; Rolandi, R.; Morgante, A.; Floreano, L.; M., C. *J. Phys. Chem. B* **2005**, *109*, 18003–18009.
(36) Barlow, S. M.; Kitching, K. J.; Haq, S.; Richardson, N. V. *Surf. Sci.* **1998**, *401*, 322–335.

(37) Kang, J. H.; Toomes, R. L.; Polcik, M.; Kittel, M.; Hoeft, J. T.; Efstathiou, V.; Woodruff, D. P.; Bradshaw, A. M. *J. Chem. Phys.* **2003**, *118*, 6059–6071.
(38) Sayago, D. I.; Polcik, M.; Nisbet, G.; Lamont, C. L. A.; Woodruff, D. P. *Surf. Sci.* **2005**, *590*, 76–87.
(39) Chen, Q.; Frankel, D. J.; Richardson, N. V. *Surf. Sci.* **2002**, *497*, 37–46.
(40) Rankin, R. B.; Sholl, D. S. *Surf. Sci.* **2004**, *548*, 301–308.
(41) Rankin, R. B.; Sholl, D. S. *Surf. Sci.* **2005**, *574*, L1–L8.
(42) Zhao, X. *J. Am. Chem. Soc.* **2000**, *122*, 12584–12585.
(43) Kanazawa, K.; Taninaka, A.; Takeuchi, O.; Shigekawa, H. *Phys. Rev. Lett.* **2007**, *99*, 216102.
(44) Chen, Q.; Richardson, N. V. *Prog. Surf. Sci.* **2003**, *73*, 59–77.
(45) Pascual, J. I.; Barth, J. V.; Ceballos, G.; Trimarchi, G.; De Vita, A.; Kern, K.; Rust, H. P. *J. Chem. Phys.* **2004**, *120*, 11367–11370.
(46) Wagner, T.; Bannani, A.; Bobisch, C.; Karacuban, H.; Moller, R. *J. Phys.: Condensed Matter* **2007**, *19*, 056009.
(47) Barth, J. V.; Behm, R. J.; Ertl, G. *Surf. Sci.* **1995**, *341*, 62–91.
(48) Allinger, N. L. *J. Am. Chem. Soc.* **1977**, *99*, 8127–8134.
(49) Pennec, Y.; Auwarter, W.; Schiffrin, A.; Weber-Bargioni, A.; Riemann, A.; Barth, J. V. *Nat. Nanotechnol.* **2007**, *2*, 99–103.
(50) Hyldgaard, P.; Persson, M. *J. Phys.-Condensed Matter* **2000**, *12*, L13–L19.
(51) Schiffrin, A.; Reichert, J.; Auwarter, W.; Jahnz, G.; Pennec, Y.; Weber-Bargioni, A.; Stepanyuk, V. S.; Niebergall, L.; Bruno, P.; Barth, J. V. *Phys. Rev. B* **2008**, *78*, 035424.
(52) Repp, J.; Moresco, F.; Meyer, G.; Rieder, K. H.; Hyldgaard, P.; Persson, M. *Phys. Rev. Lett.* **2000**, *85*, 2981–2984.
(53) Knorr, N.; Brune, H.; Epple, M.; Hirstein, A.; Schneider, M. A.; Kern, K. *Phys. Rev. B* **2002**, *65*, 115420.
(54) Silly, F.; Pivetta, M.; Ternes, M.; Patthey, F.; Pelz, J. P.; Schneider, W. D. *Phys. Rev. Lett.* **2004**, *92*, 016101.
(55) Stepanyuk, V. S.; Negulyaev, N. N.; Niebergall, L.; Longo, R. C.; Bruno, P. *Phys. Rev. Lett.* **2006**, *97*, 186403.
(56) Lukas, S.; Witte, G.; Woll, C. *Phys. Rev. Lett.* **2002**, *88*, 028301.
(57) Blankenburg, S.; Schmidt, W. G. *Phys. Rev. B* **2008**, *78*, 233411–233414.
(58) Crommie, M. F.; Lutz, C. P.; Eigler, D. M. *Nature* **1993**, *363*, 524–527.

JP900593G